Quantitative investigation of two metallohydrolases by X-ray absorption spectroscopy near-edge spectroscopy."

ARTICLE *in* NUCLEAR INSTRUMENTS AND METHODS IN PHYSICS RESEARCH SECTION A ACCELERATORS SPECTROMETERS DETECTORS AND ASSOCIATED EQUIPMENT · SEPTEMBER 2007

Impact Factor: 1.22 · DOI: 10.1016/j.nima.2007.05.196

Available online at www.sciencedirect.com
ScienceDirect
Nuclear Instruments and Methods in Physics Research A 580 (2007) 451–456
NUCLEAR INSTRUMENTS & METHODS IN PHYSICS RESEARCH Section A
www.elsevier.com/locate/nima

Quantitative investigation of two metallohydrolases by X-ray absorption spectroscopy near-edge spectroscopy

W. Zhao[a], W.S. Chu[b], F.F. Yang[b], M.J. Yu[b], D.L. Chen[b], X.Y. Guo[b], D.W. Zhou[a], N. Shi[a], A. Marcelli[c], L.W. Niu[a], M.K. Teng[a], W.M. Gong[d], M. Benfatto[c], Z.Y. Wu[b,c,*]

[a]*Hefei National Laboratory for Physical Sciences at Microscale and School of Life Sciences, University of Science and Technology of China, Hefei, Anhui 230027, China*
[b]*Institute of High Energy Physics, Chinese Academy of Sciences, Beijing 100049, China*
[c]*Istituto Nazionale di Fisica Nucleare, Laboratori Nazionali di Frascati, P.O. Box 13, Frascati 00044, Italy*
[d]*Institute of Biophysics, Chinese Academy of Sciences, Beijing 100101, China*

Available online 18 May 2007

Abstract

The last several years have witnessed a tremendous increase in biological applications using X-ray absorption spectroscopy (BioXAS), thanks to continuous advancements in synchrotron radiation (SR) sources and detector technology. However, XAS applications in many biological systems have been limited by the intrinsic limitations of the Extended X-ray Absorption Fine Structure (EXAFS) technique e.g., the lack of sensitivity to bond angles. As a consequence, the application of the X-ray absorption near-edge structure (XANES) spectroscopy changed this scenario that is now continuously changing with the introduction of the first quantitative XANES packages such as Minut XANES (MXAN). Here we present and discuss the XANES code MXAN, a novel XANES-fitting package that allows a quantitative analysis of experimental data applied to Zn *K*-edge spectra of two metalloproteins: *Leptospira interrogans* Peptide deformylase (*Li*PDF) and acutolysin-C, a representative of snake venom metalloproteinases (SVMPs) from *Agkistrodon acutus* venom. The analysis on these two metallohydrolases reveals that proteolytic activities are correlated to subtle conformation changes around the zinc ion. In particular, this quantitative study clarifies the occurrence of the *Li*PDF catalytic mechanism via a two-water-molecules model, whereas in the acutolysin-C we have observed a different proteolytic activity correlated to structural changes around the zinc ion induced by pH variations.

PACS: 61.10.Ht; 31.15.Ar; 68.18.Fg; 75.47.Pq

Keywords: BioXAS; MXAN; XANES; Metalloprotein; *Li*PDF; acutolysin-C

1. Introduction

Metalloproteins are one of the most important classes of proteins and perform a wide variety of fundamental biological processes. Synchrotron radiation (SR) X-ray sources provide the most powerful capabilities for structure–function investigations in this class of systems that constitutes almost 35% of the proteins of the entire genome [1,2]. Metalloproteins exploit the redox and coordination chemistry of biological metals to perform a variety of chemical reactions. In order to understand how these proteins utilize the chemistry of metals to perform a specific function, it is mandatory to know their 3D structure and its metal site at a high resolution. Actually, small changes around the metal site can be amplified by the protein to perform different complex biological processes.

Although recent advances in X-ray sources and detector technologies have allowed the determination of a continuously increasing number of protein structures at atomic resolution, e.g., <1.2 Å, the number of the resolved structures remains a relatively small fraction of the total and in particular, only about 2.5% of the atomic resolution structures were found to be available in the protein data

*Corresponding author. Tel.: +86 10 88235996; fax: +86 10 885294.
E-mail address: wuzy@ihep.ac.cn (Z.Y. Wu).

0168-9002/$ - see front matter © 2007 Elsevier B.V. All rights reserved.
doi:10.1016/j.nima.2007.05.196

bank (PDB) on October 2006 containing Cu, Fe and Zn proteins [3].

X-ray absorption spectroscopy (XAS) is a powerful technique capable of determining the local structure around a photoabsorber atom [4]. It has the ability to resolve structural differences at a resolution commensurate with the different redox and coordination chemistry of the metal ion regardless of the physical state of the sample under investigation. In addition, the XAS method is really synergic with protein crystallography (PX) and nuclear magnetic resonance (NMR) techniques and the combination of these different approaches may lead to significant advances in the understanding of this specific class of proteins.

The application of the XAS technique to protein research has been named "BioXAS" and several dedicated issues have been recently published (http://journals.iucr.org/s/issues/2005/01/00/issconts.html). Early work on metalloproteins have mainly focused on the use of Extended X-ray Absorption Fine Structure (EXAFS) analysis [5,6], one of the most powerful tools for reconstructing the local structure around the active site of a metalloprotein. Widely applied due to its simple data analysis, in contrast to X-ray Absorption Near-Edge Spectroscopy (XANES), the EXAFS technique has three main drawbacks:

(i) It is difficult to get reliable EXAFS data in dilute biological systems. Indeed, the potential application of this technique is limited by (a) low concentrations of a metal ion bound to a large biomolecule e.g., concentrations ranging from iM to a few mM; (b) damping of the EXAFS oscillations owing to the structural disorder present in the metal–ion coordination sphere; (c) the weak scattering amplitudes of light elements mainly constituting these biological systems. Actually, the optimal EXAFS S/N ratio for fluorescence spectra is of the order of 10^3–10^4 while it is just 10^2 for XANES. Therefore, XANES spectra are most suitable for highly diluted biological samples.

(ii) EXAFS is sensitive only to bonding distances around the active site; excluding a few specific cases occurring in a collinear geometry, bonding angles cannot be determined by EXAFS. This technique returns information about local structures only in terms of pair distribution functions around the central atom, e.g., contributions due to single-scattering processes involving the central atom and an atom in an outer shell. On the contrary, XANES contains information about the stereochemical details, e.g., coordination geometry and bond angles which are essential in biological systems, due to multiple-scattering processes involving three or more atoms around the photoabsorber.

(iii) The lack of subtle structural differences, peculiar in the XANES spectral range but missing in the EXAFS energy range. Indeed, because the quantitative characterization of the local structure of the photoabsorber represents a specific and challenging task, the fit of the XANES part of the spectrum, i.e., from the rising edge up to few hundreds of eV, has been always a dream for the users of the method. In the last decade, at Frascati there has recently been developed a novel software package called MINUIT XANes (MXAN) in the framework of the *ab initio* full Multiple Scattering (MS) theory that is capable of performing a quantitative analysis [7,8]. This method has been successfully applied to several biological systems [9–11].

In this paper, we focus on quantitative investigation, using the XANES technique combined with the MXAN fitting package, of two important metallohydrolases: the *Leptospira interrogans* peptide deformylase (*Li*PDF) and the other is acutolysin-C, a representative of snake-venom metalloproteinases (SVMPs) from *Agkistrodon acutus* venom.

Peptide deformylase (PDF) being an essential component for normal growth of bacteria is an attractive target to develop new antibiotics [12]. Previously, a four-step catalytic mechanism, proposed by Chen et al. (1997), showed that the zinc-coordinated water molecule (Wat1) is hydrogen bonded to the nearby Gln50 residue directly [13]. Later, a five-step catalytic mechanism, proposed by Becker et al. (1998), pointed out that Wat1 is connected with Gln50 through a second water molecule (Wat2) and the Wat1-hydrogen-bonded Wat2 occupies the proper position in a substrate-binding pocket [14]. However, all of these mechanisms have been proposed on the basis of the crystallographic structures although the position of the second water molecule (Wat2) present in the solution is still not known.

L. interrogans PDF (*Li*PDF) originates from the bacterium of *Leptospira*, a ubiquitous environmental bacterium that can cause infections in both animals and humans. Although, several crystallographic structures of *Li*PDF have been resolved (PDB ID: 1Y6H for pH 3.0, 1VEV for pH 6.5, 1VEY for pH 7.0, 1SV2 for pH 7.5, 1VEZ for pH 8.0) [15,16], in this study, we investigated the local structure of the *Li*PDF zinc center by means of BioXAS. A Zn *K*-edge XANES spectrum in solution at pH 8.0, e.g., in an active state of the metallohydrolase, has been collected and analyzed.

The acutolysin-C is a member of snake venom metalloproteinases (SVMPs), characterized by a molecular mass of 22.8 kDa naturally existing in *Agkistrodon acutus* venom, that includes one zinc ion in the catalytic center. This metalloproteinase shows an endopeptidase activity and a weak hemorrhagic activity. The hemorrhagic activity is due to its hydrolytic ability to destroy the structures of capillary basement membranes after injection into the organism [17–19]. For the proteolytic characteristic, this protein displays a high activity under alkaline conditions, and possesses low or no activity under acidic condition [20]. The reason for such strong pH-dependent characteristic has been assigned to subtle structural change of the

zinc-containing catalytic center [21]. Even though its general catalytic mechanism was proposed a decade ago many details are still not understood [22–24]. Only one crystal structure of acutolysin-C has been published under pH 7.5 condition (with a resolution of 2.2 Å with the PDB entry code: 1QUA) [20]. In order to shed light on the intrinsic mechanism of acutolysin-C in solution, we have collected a series of XAS spectra of the acutolysin-C at different pH values.

2. Experiment

2.1. Preparation of LiPDF sample

Escherichia coli BL21(DE3) cells carrying plasmid pET22b-*Li*PDF were expressed as reported previously [25]. Cells were harvested by centrifugation and resuspended in 20 ml buffer A (50 mM Hepes7.5, 10 mM NaCl). After sonication, cell debris were removed by centrifugation. The supernatant (20 ml) was applied onto a HiTrapTM 5 ml Q HP (Amersham Pharmacia Biotech) column equilibrated with buffer B (50 mM Tris–HCl pH 8.5, 10 mM NaCl). The column was eluted with 250 ml buffer B plus a linear gradient of 10 mM–1 M NaCl (AKTA purifier 900, Amersham Pharmacia Biotech). The fractions with PDF activity were concentrated and then applied to a SuperdexTM 75 column (16/60, Amersham Pharmacia Biotech) pre-equilibrated with buffer C (50 mM Tris–HCl pH8.0, 50 mM NaCl).

2.2. Preparation of acutolysin-C sample

The crude venom of *Agkistrodon acutus* was obtained from the southern mountain region of the Anhui Province (China). The preparation of acutolysin-C was performed at the School of Life Sciences USTC (Hefei, China), according to the published method [21]. The purified acutolysin-C was desalted, lyophilized and further dissolved to obtain a protein concentration of 100 mg/ml into 100 mM of Glycine–HCl (pH 3.0), Mes-NaOH (pH 6.0) or Tris–HCl (pH 8.0) buffers, respectively.

2.3. XAS spectra measurement

X-ray absorption spectra at the Zn *K*-edge were collected at the X-ray absorption station (beamline 4W1B) of the Beijing Synchrotron Radiation Facility (BSRF) in the fluorescence yield mode. The storage ring was working at 2.2 GeV and experiments were performed with an electron current decreasing from 135 to 80 mA during a time span of about 8 h. The incident beam intensity was monitored using an ionization chamber flowed by a 25% argon 75% nitrogen mixture while the fluorescence signal was collected by means of a Lytle detector flowed by argon gas. The solution of the two metalloproteins was kept in a cell sealed by kapton film and Teflon spacers of 1.2 mm. Several scans for each sample were added to improve the signal-to-noise ratio. In order to explore the local structure of the two metallohydrolases in an active state, all spectra were collected at room temperature. After the XAS experiments, the proteolytic activities of all solution samples were measured repeatedly. Compared with that of the native state, the change of the proteolytic activity was small (data not shown), so that the possible X-ray damage can be considered negligible and the XAS spectra really reflect the native zinc local structures in the solution state.

3. MXAN calculations

To extract detailed structural information around the zinc ion site, we applied the software package MXAN (Minuit XANes) [26,27]. This package is capable of performing quantitative analysis of a XAS spectrum from the absorption edge up to 200 eV via a comparison of the experimental data and theoretical calculations generated by changing relevant geometrical parameters of the atomic sites [26,27]. The X-ray absorption cross-sections have been calculated using the full multiple scattering scheme in the framework of the muffin-–in (MT) approximation for the shape of the potential [28,29]. In particular, the exchange and the correlation part of the potential have been determined on the basis of the local density approximation of the self-energy. Inelastic processes were accounted for by a convolution with a broadening Lorentzian function having an energy-dependent width of the form $\Gamma(E) = \Gamma_c + \Gamma_{mfp}(E)$. The constant part Γ_c accounts for both the core–hole lifetime (1.8 eV) [30] and the experimental resolution (1.5 eV), while the energy-dependent term represents all the intrinsic and extrinsic inelastic processes [26,31,32]. The MT radii were chosen according to the Norman criterion with a 15% overlap [33,34]. The method takes into account MS events in a rigorous way through the evaluation of the scattering path operator [28,35] and its reliability has been successfully tested over the years in many different applications [26,31].

4. Results and discussion

4.1. L. interrogans peptide deformylase (LiPDF)

The local structure of the *Li*PDF active center is shown in Fig. 1— a zinc ion coordinated with one catalytic water molecule, a sulfur atom of cysteine residue and two imidazole Nε2 atoms of the histidine residues. With MXAN the Zn *K*-edge XANES of *Li*PDF has been simulated starting from the crystal structure of *Li*PDF (PDB code 1SV2, 3.0 Å resolution). The panel in Fig. 2 shows the best simulation achieved corresponding to the crystallographic data. However, significant discrepancies are evident so that, it is clear that the low-resolution crystallographic data does not allow obtaining an accurate description of the local structure around the metal site. Conversely, MXAN is able to return a better agreement with the experiments, addressing significant displacements

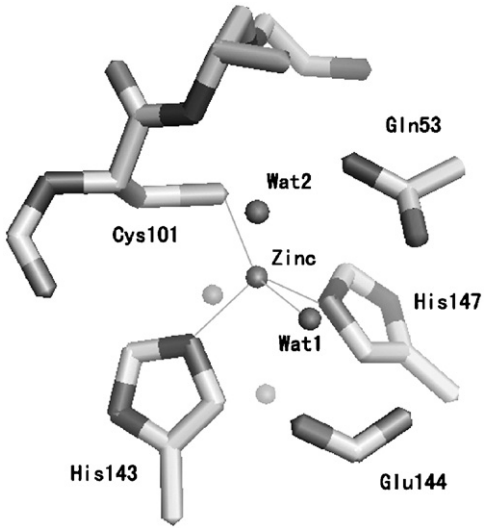

Fig. 1. The local structure of the *Li*PDF active center.

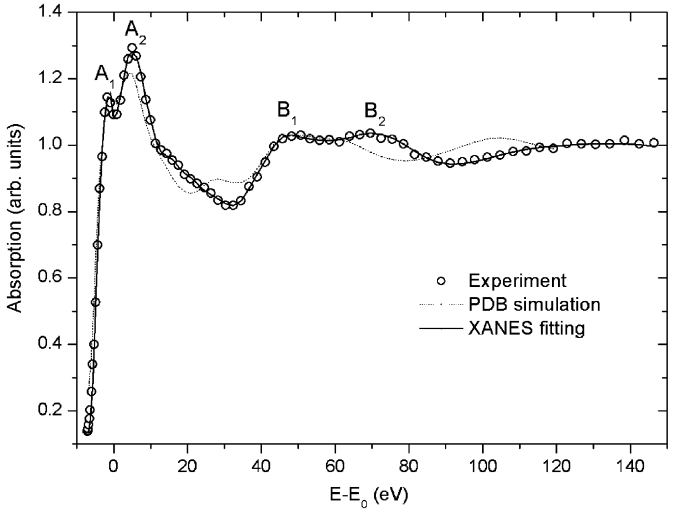

Fig. 2. Comparison between experimental data at pH 8.0 (circles), XANES simulations at the Zn *K*-edge spectrum with the crystallography structure (dashed line) and the best fit with two-water model (solid line).

of the neighboring atoms with respect to the considered structural models.

To resolve the fine structure of the *Li*PDF active center in the native state and eventually recognize the presence of Wat2, we addressed the occurrence of a structural model based on the PDB 1Y6H, in which the formate group of 1Y6H is replaced with two water molecules. The proper model–cluster size has been determined starting with an initial cluster of 19 atoms and slowly increasing its size to get convergence for the simulation with a cluster of 50 atoms within a sphere of 6.0 Å radius from the zinc center. In Fig. 2, we compare the experimental data (circles) at pH 8.0 and the best fit (solid line) of the two-water model. Spectra are characterized by four main features: A1, A2, B1 and B2. The peak A is due to the multiple scattering, up to infinite, of the excited photoelectron within a finite

Table 1
Refined critical distances of the best fits and the data of the original two-water model based on PDB 1Y6H

Atom pairs	Zn–H_{143} $N_{\varepsilon 2}$	Zn–H_{147} $N_{\varepsilon 2}$	Zn–C_{101} S_{γ}	Zn–Wat1	Zn–Wat2
Model (Å)	2.17	2.15	2.40	2.31	3.90
Fit (Å)	2.00	1.99	2.25	2.41	3.57

cluster of atoms surrounding the absorbing atom, so that it can be called a "shape resonance". The feature B is due to an EXAFS-like scattering within a cluster composed by the nearest neighboring atoms surrounding the central atom. Thus the energy position of the feature B directly correlates to the bond length of the metal atom and the nearest neighboring atoms [36]. The split of the features A and B indicates that there are two or more scattering contributions of the bond distances between the central atom and the nearest neighboring atoms. The best agreement between the experimental data of the native state and the best fit refers to the two-water model. The relevant refined critical distances of the best fit are listed in Table 1 together with the data of the original model. In fact, our XANES fitting provides direct evidence for the state in the first step of the five-step catalytic mechanism, as proposed by the crystallographic structures of the *E. coli* PDF [14]. That is, the local structure returned by MXAN indicates that in the substrate-free solution state a second water molecule (Wat2) occupies the proper position in substrate binding pocket.

4.2. Acutolysin-C

It has been proposed that the pH-dependent characteristics of SVMPs are due to structural subtle changes in the catalytic center [21]. Indeed, three XANES spectra of acutolysin-C measured under different chemical environments from acidic to alkaline pH values show significant differences (Fig. 3A), which could be attributed to structural local changes around the catalytic center of acutolysin-C. The spectrum measured under pH 6.0 contains double peaks in the energy region of 9660–9670 eV, similar to that observed at pH 8.0, a result consistent with the result that acutolysin-C displays proteolytic activities at both pH values while a weak activity occurs at pH 6.0. However, in contrast to these two profiles, the other curve recorded under pH 3.0 displays more significant differences with only one main peak at the energy 9665 eV. It probably indicates that some local structure changes correlated with the absence of the activity when pH decreases to 3.0.

For the MXAN analysis of acutolysin-C, we used a cluster of 41 atoms within a radius of 6 Å from the zinc ion. The initial model of the cluster has been based on the crystal structure, recrystallized under the same condition as reported previously [20] and resolved with a resolution of 1.9 Å (private communication). Based on the method described above, we first started the XANES fit at the

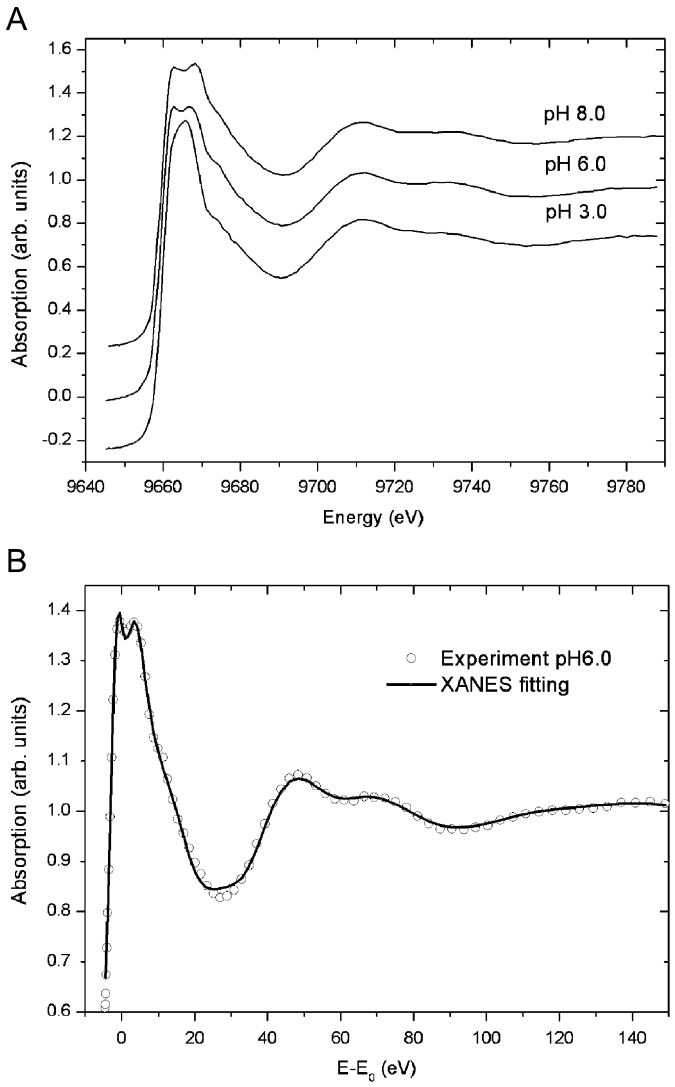

Fig. 3. (A): The Zn *K*-edge XANES spectra of acutolysin-C measured under the experimental conditions with different pH values. (B): Comparison between the Zn *K*-edge XANES experimental data (circles) and the fit (solid line) of the acutolysin-C at pH 6.0.

pH 6.0 spectrum to rebuild the local structure around the photoabsorber. As shown in Fig. 3B, a good agreement between the experimental profile and the fit has been reached, while some additional structural parameters were obtained (Table 2). Comparing the bonding distances at pH 6.0 obtained by fit with that at pH 7.5 from previous PX data, we find that zinc clusters change going from pH 7.5 to 6.0 conditions. The quantitative MXAN analysis shows that when pH decreases from pH 7.5 to 6.0 (Table 2), the distance between the catalytic water molecule and the zinc ion (Wat1-zinc) increases, e.g., from 2.29 to 2.55 Å. Moreover, the distance of the first shell atoms, between the three imidazole Nε2 atoms of the histidines and the zinc ion, decreases down to about 0.03 Å. Because of the limit of the PX method, the 0.03 Å change falls in the error-range of the crystallographic structure of 2.20 Å e.g., a resolution with an Rfree value of 27.2% [20]. However, it is not clear

Table 2
Comparison of the most relevant distances returned by the XANES fit at pH 6.0 and the protein X-ray crystallographic data of acutolysin-C at pH 7.5

Atom Pairs	Zn–H_{142} $N_{\varepsilon 2}$	Zn–H_{146} $N_{\varepsilon 2}$	Zn–H_{152} $N_{\varepsilon 2}$	Zn-Wat1
PDB 1QUA (Å)	2.08	2.07	2.10	2.29
Fit (Å)	2.06	2.04	2.05	2.55

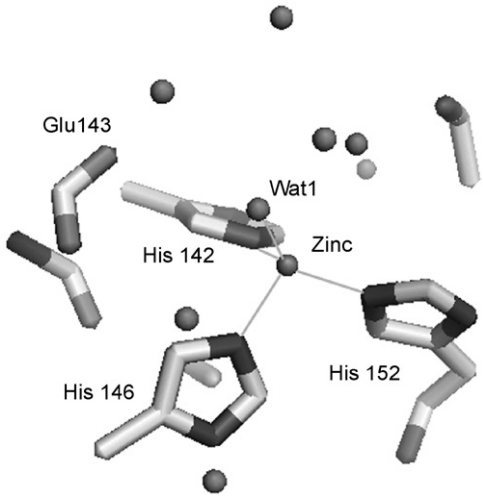

Fig. 4. The local structure of acutolysin-C for the XANES analysis.

yet whether the distances between the first shell atoms and the zinc ion change when the pH value is altered.

The local structure of acutolysin-C around the zinc ion (Fig. 4) shows that this metal ion is coordinated in a tetrahedral manner with one catalytic water molecule (Wat1) and three imidazole Nε2 atoms (His142, His146, His152). Furthermore, Wat1 acts as the reagent of the nucleophilic attack during the proteolytic reaction. The observed changes of proteolytic activity along with different pH values are related to the catalytic water molecule, in which Wat1 is polarized by the zinc ion and the carboxylate group of nearby Glu143 residue. The increased Wat1–zinc distance indicates that the polarization degree of Wat1 from the zinc ion decreases, which may be the reason for the decrease in the catalytic activity of acutolysin-C from pH 7.5 to 6.0.

5. Conclusion

Comparison between EXAFS and XANES analysis may address exact and more detailed steoro-geometry information, especially suitable for dilute biologic samples. The relation between the local structure around the metal site and biological functions in the two metallohydrolases has been studied using the XANES technique and *ab initio* calculation. The results reveal that the proteolytic activities are correlated with subtle conformational changes around the zinc ion. Furthermore, a quantitative XANES

investigation elucidated that *Li*PDF acquires a catalytic activity through a two-water-molecules model, whereas, acutolysin-C shows different proteolytic activities related with the distances between the atoms around the zinc ion alone with the alteration of pH condition. However, some mechanisms are not clear yet, e.g., the acid-inactive mechanism of acutolysin-C, and this work is in progress and will be addressed in a forthcoming paper.

Acknowledgments

Sincere thanks are due to Drs. Yiwei Liu and Ziqiang Zhu for their help in sample preparation and helpful discussions. Z. W. acknowledges the financial support of the Key Development Project of the Chinese Academy of Sciences (KJCX-SW-N06), the National Outstanding Youth Fund (N.10125523) and the Key Important Project of the National Natural Science Foundation of China (Grant nos. 10490190 and 10490191).

References

[1] S.J. Lippard, J.M. Berg, Principles of Bioinorganic Chemistry, University Science Books, Sausalito, 1994.
[2] H.A.O. Hill, P.J. Sadler, A.J. Thomson, Metal Sites in Proteins and Models, Springer, Berlin, 1999.
[3] S.S. Hasnain, K.O. Hodgson, J. Synchrotron Radiat. 6 (1999) 852.
[4] D.C. Koningsberger, R. Prins, X-ray Absorption: Principle, Applications, Techniques of EXAFS, SEXAFS and XANES, Wiley, New York, 1998.
[5] T.E. Wolff, J.M. Berg, C. Warrick, K. Hodgson, R.H. Holm, J. Am. Chem. Soc. 100 (1978) 4630.
[6] J.E. Pennerhahn, R.M. Fronko, V.L. Pecoraro, C.F. Yocum, S.D. Betts, N.R. Bowlby, J. Am. Chem. Soc. 112 (1990) 2549.
[7] M. Benfatto, A. Congiu-Castellano, A. Daniele, S. Della Longa, J. Synchrotron Radiat. 8 (2001) 267.
[8] P. Frank, M. Benfatto, R.K. Szilagyi, P. D'Angelo, S. Della Longa, K.O. Hodgson, Inorg. Chem. 44 (2005) 1922.
[9] M. Benfatto, S. Della Longa, Y. Qin, Q. Li, G. Pan, Z. Wu, S. Morante, Biophys. Chem. 110 (2004) 191.
[10] K. Hayakawa, K. Hatada, P. D'Angelo, S. Della Longa, C.R. Natoli, M. Benfatto, J. Am. Chem. Soc. 126 (2004) 15618.
[11] S. Li, Z. Zhou, W. Chu, W. Gong, M. Benfatto, T. Hu, Y. Xie, D. Xian, Z. Wu, J. Synchrotron Radiat. 12 (2005) 111.
[12] P.T.R. Rajagopalan, X.C. Yu, D.H. Pei, J. Am. Chem. Soc. 119 (1997) 12418.
[13] M.K. Chan, W. Gong, P.T. Rajagopalan, B. Hao, C.M. Tsai, D. Pei, Biochemistry 36 (1997) 13904.
[14] A. Becker, I. Schlichting, W. Kabsch, D. Groche, S. Schultz, A.F. Wagner, Nat. Struct. Biol. 5 (1998) 1053.
[15] Z. Zhou, X. Song, Y. Li, W. Gong, J. Mol. Biol. 339 (2004) 207.
[16] Z. Zhou, X. Song, W. Gong, J. Biol. Chem. 280 (2005) 42391.
[17] C.L. Ownby, Locally Acting Agents: Myotoxins, Hemorrhagic Toxins and Dermonecrotic Factors, Marcel Dekker, New York, 1990.
[18] H. Ta keya, S. Iwanaga, Proteases that Induce Hemorrhage, Alaken, Colorado, 1998.
[19] J.M. Gutierrez, A. Rucavado, Biochimie 82 (2000) 841.
[20] X. Zhu, M. Teng, L. Niu, Acta Crystallogr. D 55 (1999) 1834.
[21] W. Gong, X. Zhu, S. Liu, M. Teng, L. Niu, J. Mol. Biol. 283 (1998) 657.
[22] S. Kunugi, H. Hirohara, N. Ise, Eur. J. Biochem. 124 (1982) 157.
[23] B.W. Matthews, Acc. Chem. Res. 21 (1988) 333.
[24] F. Grams, V. Dive, A. Yiotakis, I. Yiallouros, S. Vassiliou, R. Zwilling, W. Bode, W. Stocker, Nat. Struct. Biol. 3 (1996) 671.
[25] Y. Li, S. Ren, W. Gong, Acta Crystallogr. 58 (2002) 846.
[26] S.D. Longa, A. Arcovito, M. Girasole, J.L. Hazemann, M. Benfatto, Phys. Rev. Lett. 87 (2001) 155501.
[27] A. Cardelli, G. Cibin, M. Benfatto, S. Della Longa, M.F. Brigatti, A. Marcelli, Phys. Chem. Miner. 30 (2003) 54.
[28] C.R. Natoli, M. Benfatto, J. Phys. (Paris) Colloq. 47 (C8) (1986) 11.
[29] Z.Y. Wu, G. Ouvrard, S. Lemaux, P. Moreau, P. Gressier, F. Lemoigno, J. Rouxel, Phys. Rev. Lett. 77 (1996) 2101.
[30] J.C. Fuggle, J.E. Inglesfield, Top. Appl. Phys. 69 (1992) 1.
[31] M. Benfatto, S. Della Longa, C.R. Natoli, J. Synchrotron Radiat. 10 (2003) 51.
[32] O.M. Roscioni, P. D'Angelo, G. Chillemi, S. Della Lonaga, M. Benfatto, J. Synchrotron Radiat. 12 (2005) 75.
[33] J.G. Norman, Mol. Phys. 81 (1974) 1191.
[34] Y. Joly, Phys. Rev. B 63 (2001) art. no.
[35] Z.Y. Wu, D.C. Xian, C.R. Natoli, A. Marcelli, E. Paris, A. Mottana, Appl. Phys. Lett. 79 (2001) 1918.
[36] Z.Y. Wu, S. Gota, F. Jollet, M. Pollak, M. GautierSoyer, C.R. Natoli, Phys. Rev. B 55 (1997) 2570.